Norbornadiene-Based Molecules for Functionalizing The Si(001) Surface

ARTICLE *in* THE JOURNAL OF PHYSICAL CHEMISTRY C · SEPTEMBER 2009

Impact Factor: 4.77 · DOI: 10.1021/jp903481w

ohio2/yjy-yjy/yjy-yjy/yjy99907/yjy9839d07z | xppws | 23:ver.3 | 8/7/09 | 15:41 | Msc: jp-2009-03481w | TEID: ccd00 | BATID: 00000

Norbornadiene-Based Molecules for Functionalizing The Si(001) Surface

Sherin A. Saraireh,[†] Phillip V. Smith,*[,†] Bruce V. King,[†] Jeffrey R. Reimers,[‡] Brian J. Wallace,[‡] and Maxwell J. Crossley[‡]

School of Mathematical & Physical Sciences, University of Newcastle, Callaghan, NSW 2308, Australia, and School of Chemistry, The University of Sydney, NSW 2006, Australia

Received: April 16, 2009; Revised Manuscript Received: July 15, 2009

One of the fundamental requirements in the development of silicon-based molecular electronic devices is the ability to attach organic molecules to silicon surfaces to form well-defined structures that are stable and possess specific characteristics. Previous work has shown that, although norbornadiene (NBE) forms very stable structures on the Si(001) surface with its apex CH_2 group pointing outward from the surface, these structures cannot be resolved in scanning tunneling microscopy. In this paper, we report the results of density functional theory calculations of the interaction with the Si(001) surface of 7-trifluoroacetoxy-norbornadiene (7-TFA-NBE) in which a hydrogen atom of the apex CH_2 group is substituted by the trifluoroacetoxy $OC(O)CF_3$ group. This molecule is shown to form very stable structures with the trifluoroacetoxy group sitting well above the surface. Moreover, in contrast to NBE, we find that the different 7-TFA-NBE chemisorption structures should be distinguishable in high-resolution scanning tunneling microscopy experiments. This raises the exciting possibility of employing norbornadiene-based molecules with appropriately chosen functional groups to create molecular structures on Si(001) that are stable and experimentally distinguishable and yield the requisite atomic and electronic properties.

1. Introduction

The functionalization of semiconductor surfaces via the chemisorption of organic molecules has the potential to create new technologies that utilize the best properties of both organic and inorganic materials. One of the most important potential applications of the functionalization of a semiconductor surface is that of molecular electronics and its integration into the existing silicon-based technology.[1] The prospect that this raises of obtaining significantly enhanced miniaturization has prompted extensive studies of the interaction and properties of many different organic molecules on silicon surfaces.[2−6] Employing silicon surfaces as the basis for single-molecule electronic devices is particularly attractive[7] because organic molecules, which are carbon-based, should form strong bonds with a silicon surface without any intermediate species. This should be especially true for the Si(001) surface as it has a relatively high density of dangling bonds and, hence, is quite reactive to incident molecules. To date, the interactions of many different organic molecules with the Si(001) surface have been studied.[6−18] Despite all of this work, however, the problem still remains of finding molecules that display the requisite properties for molecular electronics applications and are stable under typical I−V working conditions.[19]

It has been shown that norbornadiene (NBE) (systematic name is bicyclo[2.2.1]hepta-2,5-diene; see Figure 1a),[20] can be selectively chemisorbed on Si to produce templates for nanopatterning.[21−23] Density functional theory (DFT) calculations[24] modeling the adsorption of NBE on the clean Si(001) surface have predicted that norbornadiene will form adsorbate structures on the Si(001) surface that are characterized by four Si−C bonds and, hence, are very stable. Moreover, its CH_2 group is predicted to sit at the apex of each adsorbate structure pointing outward from the surface. This suggests that very stable molecular adsorbate structures with specific characteristics on the Si(001) surface could be obtained by employing other norbornadiene-based molecules in which the CH_2 group of NBE has been replaced by appropriately chosen functional groups.

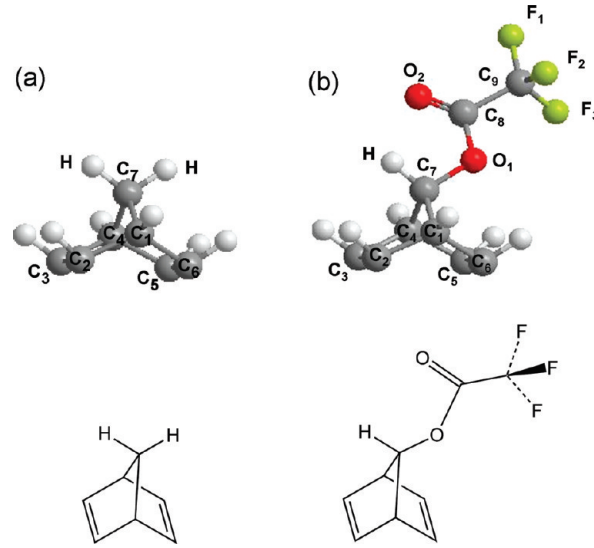

Figure 1. Schematics of the (a) norbornadiene molecule and (b) 7-trifluoroacetoxy-norbornadiene molecule.

STM measurements have shown that, at low coverage, NBE adopts more than one bonding configuration on the Si(001) surface,[22,23,25,26] with the chemisorbed molecules being observed centered on top of a silicon-dimer row as well as in the troughs between dimer rows. The precise bonding configurations have not been determined experimentally, however, as the informative

* To whom correspondence should be addressed. E-mail: phil.smith@newcastle.edu.au. Phone: 61-2-49-215435. Fax: 61-2-49-216907.
[†] University of Newcastle.
[‡] The University of Sydney.

10.1021/jp903481w CCC: $40.75

ohio2/yjy-yjy/yjy-yjy/yjy99907/yjy9839d07z | xppws | 23:ver.3 | 8/7/09 | 15:41 | Msc: jp-2009-03481w | TEID: ccd00 | BATID: 00000

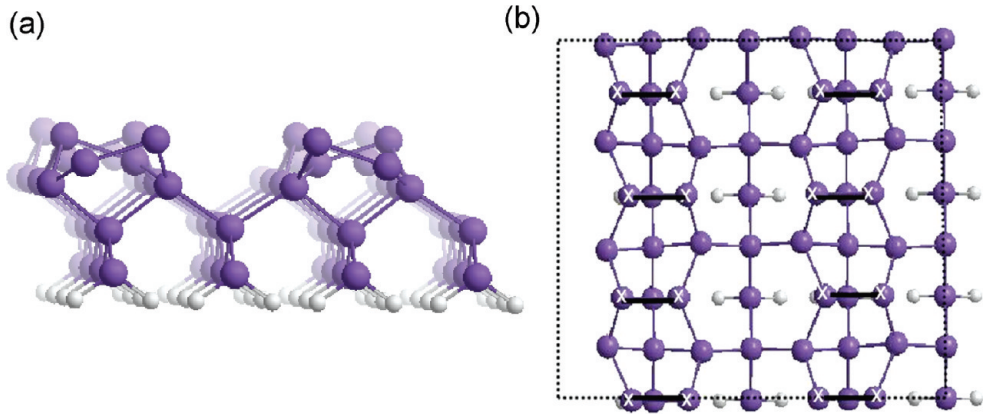

Figure 2. (a) Side view of the four-layer (4 × 4) silicon slab used to study the chemisorption of the 7-trifluoroacetoxy-norbornadiene molecule on the Si(001) surface using VASP. (b) Top view of the Si(001) (4 × 4) SUC. The dotted lines represent the (4 × 4) SUC, the white crosses indicate the top-layer silicon dimer atoms, and the solid lines between them represent the dimer bonds.

apex CH_2 group (see Figure 1a) is not well-resolved in the STM images.[22] Further, at high coverage, the STM images show a disordered arrangement of molecules,[25] suggesting that various bonding configurations for each of the above-trough and above-row chemisorbates could exist. Having several potential structures that cannot be resolved by STM is clearly not a desirable situation for molecular electronics applications where one would prefer to have a single, well-characterized structure. Replacing the CH_2 group of NBE with a larger entity could, however, allow these structures to be discriminated and characterized in STM. The ability to distinguish the different possible structures would also enable procedures to be employed to ensure that just one of these structures persisted on the surface.

In this paper, we test these ideas by investigating the interaction of one such norbornadiene-based molecule with the Si(001) surface. This is the 7-trifluoroacetoxy-norbornadiene (bicyclo[2.2.1]hepta-2,5-dien-7-ol trifluoroacetic acid ester)[27,28] molecule shown in Figure 1b. In this molecule, which we shall subsequently refer to as 7-TFA-NBE, a hydrogen from the apex CH_2 group of NBE is substituted by the trifluoroacetoxy group $OC(O)CF_3$. The issues we seek to address are the following: (i) Will the functionalization alter (improve or otherwise) the irregular kinetics-controlled growth of NBE−Si(001) monolayers? (ii) Will the trifluoroacetoxy group be unreactive with the surface or are additional adducts possible? (iii) Will the trifluoroacetoxy group preserve its chemical nature after chemisorption? (iv) Will atomic-level details concerning the binding be directly discernible from STM images, a process not possible for NBE?

2. Methods

Calculations have been performed using two different theoretical methods, the Vienna ab initio simulation package (VASP)[29−31] and Gaussian03.[32] VASP uses an iterative method to self-consistently solve the Kohn−Sham equations of density functional theory (DFT) expressed in a plane-wave basis. The electron−ion interactions are described by ultrasoft pseudopotentials of the Vanderbilt type[33,34] and the exchange and correlation contributions by the generalized gradient approximation (GGA) of Perdew and Wang (PW91).[35,36] Gaussian03, on the other hand, is an ab initio molecular-orbital method employing a localized atomic orbital basis set.

To determine the geometry of the 7-TFA-NBE molecule using VASP, we have employed a large unit cell of dimensions 15.43 Å × 15.43 Å × 20 Å. The Brillouin zone (BZ) integrations were performed using the (2 × 2 × 1) *k*-point set of Monkhorst and Pack.[37] To optimize the geometry of the molecule using Gaussian03, we first performed a restricted Hartree−Fock (RHF) calculation with the STO-3G basis set and then used this optimized RHF/STO-3G geometry to perform a more accurate UHF geometry optimization using the PW91 exchange and correlation functional[35,36] with the 6-311G(d) basis set. Optimization of the geometry of the molecule was also carried out using the B3LYP exchange and correlation functional[38] and the 3-21G* basis set.

To study the interaction of the 7-TFA-NBE molecule with the Si(001) surface using the VASP code, we have employed a (4 × 4) periodic slab unit cell (SUC) containing four atomic layers (see Figure 2) and a vacuum region of approximately 10 Å; some test calculations were also performed using up to six atomic layers. The bottom layer silicon atoms were terminated with hydrogen atoms. The BZ integrations were again performed using the Monkhorst−Pack (2 × 2 × 1) *k*-point set. The silicon lattice constant was taken to be 5.455 Å, which is the equilibrium lattice constant determined by the VASP code for bulk silicon using US pseudopotentials and PW91 exchange and correlation. The minimum-energy structures were determined by allowing all the coordinates of the molecule and the top three layers of silicon to relax.

To study the interaction of the molecule with the silicon surface using the Gaussian molecular orbital program, we have employed a $Si_{36}H_{34}$ cluster containing four layers of silicon with all of the boundary silicon atoms saturated by hydrogen. This cluster is shown in Figure 3. The B3LYP exchange and correlation functional and the 3-21G* basis set have been employed for these calculations. In these Gaussian optimization calculations, all of the atoms in the molecule and the top two layers of the silicon substrate were allowed to relax. Several different starting geometries were employed to determine the lowest-energy structure.

The STM images have been simulated from our VASP calculations using the Tersoff−Hamann approximation.[39,40] In this approximation, the intensity of a constant current STM image for bias voltage V is modeled by integrating the local density of states function over a range of energy (eV) from the Fermi energy. Our simulated STM images thus correspond to *xyz* plots in which the height z associated with mapping out a selected isodensity surface is converted into a greyscale.

3. Results

A. Determination of the Energy Cutoff. The default energy cutoffs for the oxygen and fluorine pseudopotentials in VASP

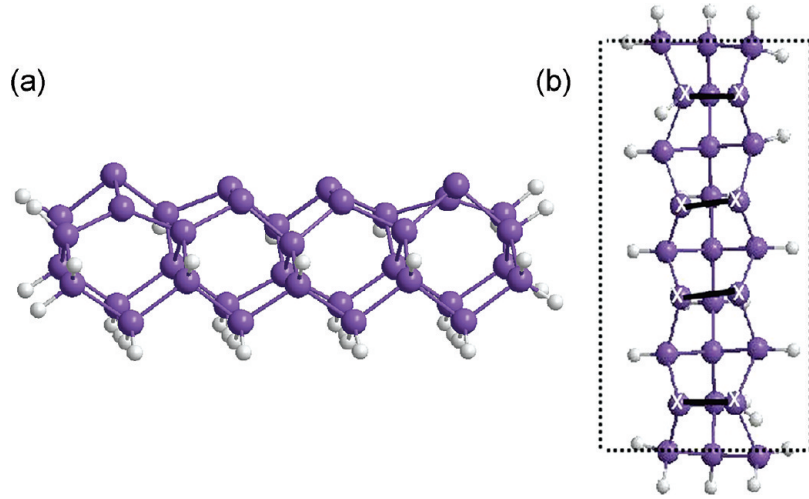

Figure 3. (a) Side view of the $Si_{36}H_{34}$ cluster used to study the interaction of the 7-trifluoroacetoxy-norbornadiene molecule on Si(001) using Gaussian03. (b) Top view of the silicon cluster in (a). The dotted lines represent the (2 × 4) SUC, whereas the white crosses and the solid lines between them represent the top-layer dimer atoms and the dimer bonds, respectively.

are both very high, thus demanding excessive computer resources. To make the calculations with our large periodic slab unit cell more tractable, we first carried out an extensive set of calculations to determine energy cutoff values that provided an acceptable balance between accuracy and computing time.

These cutoff calculations were done using the molecules methylfluoroform (CH_3CF_3), to test the fluorine−carbon interactions, and carbon dioxide (CO_2), to test the oxygen−carbon interactions. The geometries of these two molecules were optimized using cutoff energies ranging from 275 to 424 eV for CH_3CF_3 and from 200 to 424 eV for CO_2. We found that an energy cutoff of 275 eV provided a good description of both molecules, with all of the bond angles reproduced to an accuracy of better than 0.7° with respect to the corresponding values obtained using the default cutoff values. The bond lengths were also accurate to within 0.004 and 0.007 Å for CH_3CF_3 and CO_2, respectively.

To further test this cutoff value of 275 eV, we carried out binding energy calculations for one of the fluorine−carbon single bonds in CH_3CF_3 and for the oxygen−carbon double bond in CO_2. We found that the strength of the fluorine−carbon bond was predicted to be 5.99 eV, using the cutoff of 275 eV, compared with 5.71 eV, using the default value for this system of 424 eV. The energy needed to remove the first oxygen atom from CO_2 was found to be 6.37 eV, using the cutoff of 275 eV, just 0.1 eV less than the value of 6.47 eV obtained using the default cutoff of 393 eV for a system containing only carbon and oxygen atoms. The energy needed to remove the second oxygen atom was predicted to be 12.58 eV, using the 275 eV cutoff energy, compared to 12.62 eV for the default value. All of these binding energy values are consistent with experimental and theoretical values previously reported in the literature.[41−44] As an additional test of this cutoff value, we carried out a geometry optimization calculation for the 7-TFA-NBE molecule in which we let only the $OC(O)CF_3$ atomic positions relax. We found that the bond lengths and bond angles of this portion of the molecule obtained using the cutoff energy of 275 eV varied by less than 0.001 Å and 1°, respectively, from the corresponding values obtained by performing exactly the same calculation with the default cutoff values of the system.

B. Optimization of the 7-Trifluoroacetoxy-norbornadiene Molecule. To optimize the geometry of the 7-TFA-NBE molecule, we carried out VASP calculations in which all the atoms in the molecule were allowed to relax relative to one fixed atom. The results of these calculations, which were performed with the energy cutoff of 275 eV, are presented in row A of Table 1. Gaussian03 calculations were also carried out using both the PW91 exchange and correlation functional with the 6-311G(d) basis set (row B, Table 1) and the B3LYP functional with the 3-21G* basis set (row C, Table 1). Comparing the results in rows A, B, and C of Table 1, we observe that the geometries obtained using VASP and Gaussian03 are in very good agreement. The bond lengths and bond angles of the norbornadiene moiety of the 7-TFA-NBE molecule are also found to agree with the corresponding experimental and theoretical results for the NBE molecule to within 0.02 Å and 1°, respectively.[20,24] To determine whether any other geometry might be more stable than this structure, we took the geometry in row B (Table 1) as our starting geometry, varied some of the important bond lengths and bond angles, and then reoptimized the structures. We found that all of these different configurations came back to the original structure. It should be noted that the optimized geometry of the 7-TFA-NBE molecule presented in Figure 1 and Table 1 is for the conformer for which the $H-C_7-O_1-C_8$ dihedral angle is negative. There is also a second conformer for which this dihedral angle has a positive value.

C. Interaction of the 7-Trifluoroacetoxy-norbornadiene Molecule with the Si(001) Surface. To determine the most energetically favorable structures for the intact adsorption of the 7-TFA-NBE molecule on the Si(001) surface, we have studied three different scenarios. The first scenario involved coupling of the molecule to the surface via one or more of its fluorine atoms. The second involved bonding of the molecule to the surface through the oxygen atom, which makes a double bond with the carbon atom (oxygen, O_2, in Figure 1b), and the third scenario involved adsorption of the molecule via the carbon atoms in the NBE moiety. Previous work on NBE[24] and *N*-trimethylsilyl-7-azanorbornadiene (TMSAN)[45] has provided clear evidence that 7-TFA-NBE will form stable structures by the third scenario. To determine whether stable structures can be obtained, which involve bonding to the surface by the fluorine or oxygen atoms, we have carried out a range of calculations using Gaussian03 with B3LYP/3-21G*. This method was chosen as calculations using the $Si_{36}H_{34}$ substrate cluster shown in

TABLE 1: Bond Lengths (in Å) and Bond Angles (in Degrees) for the Isolated 7-TFA-NBE Molecule Using (A) VASP, (B) Gaussian03 with PW91/6-311G(d), and (C) Gaussian03 with B3LYP/3-21G*. The Atom Labeling Is the Same as in Figure 1b

	$(C-C)_{avg}$[a]	$(C=C)_{avg}$[a]	C_1-C_7	C_7-O_1	O_1-C_8	$C_8=O_2$
A	1.54	1.34	1.55	1.47	1.34	1.21
B	1.55	1.34	1.56	1.48	1.36	1.22
C	1.54	1.34	1.55	1.46	1.34	1.21
	C_8-C_9	$(C_9-F)_{avg}$[a]	$H-C_7$	$H-C_1$	$H-C_2$	$C_1-C_2-C_3$
A	1.56	1.36	1.09	1.09	1.08	107.3
B	1.53	1.37	1.09	1.09	1.08	107.6
C	1.55	1.35	1.09	1.09	1.09	107.3
	$C_6-C_1-C_2$	$C_1-C_7-C_4$	$C_7-O_1-C_8$	$O_1-C_8-O_2$	$O_2-C_8-C_9$	$O_1-C_8-C_9$
A	108.0	93.1	117.0	128.7	123.0	108.4
B	106.8	93.3	116.5	126.5	125.2	108.2
C	108.0	93.1	115.5	127.7	123.3	109.0
	$H_1-C_7-O_1$	$O_1-C_7-C_1$	$O_1-C_7-C_4$	$(H-C=C)_{avg}$[a]	$(H-C-C)_{avg}$[a]	$H-C_1-C_7$
A	108.3	111.0	115.4	128.4	116.5	117.3
B	109.2	110.1	115.7	128.1	117.1	117.4
C	108.3	111.0	115.8	128.2	116.6	117.1

[a] $(C-C)_{avg}$ and $(C=C)_{avg}$ denote the average values of all the single and double bonds, respectively, within the NBE moiety of the molecule. The other values denoted by "avg" have been averaged over all of the corresponding bond lengths and bond angles.

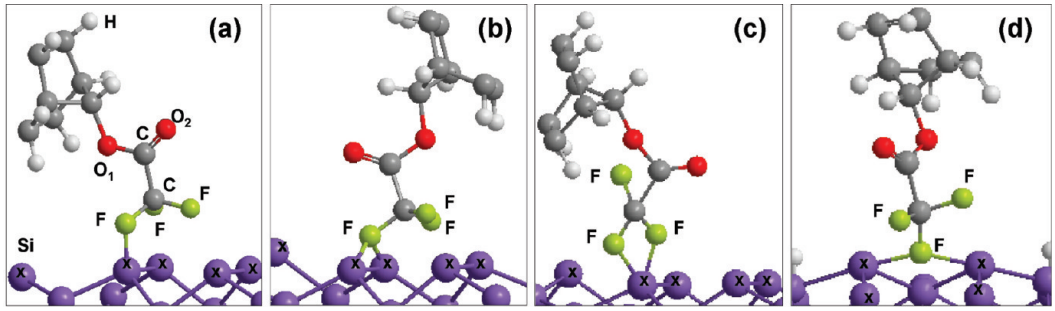

Figure 4. Different initial structures for the interaction of the 7-TFA-NBE molecule with the Si(001) surface via one or more of its fluorine atoms. The silicon dimer atoms are indicated by crosses.

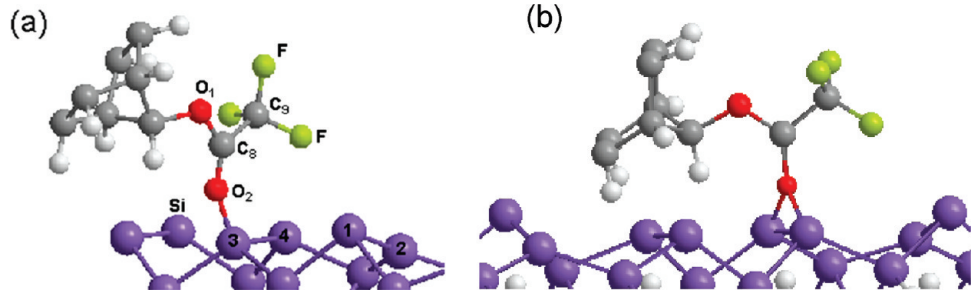

Figure 5. Starting geometries for the interaction of the 7-TFA-NBE molecule with the Si(001) surface via one of its oxygen atoms. (a) The oxygen atom makes a single bond with one of the silicon dimer atoms. (b) The oxygen atom bonds with the two silicon atoms of a single dimer.

Figure 3a are much faster than VASP geometry optimization calculations using a (4 × 4) SUC. Such considerations are essential where a significant number of different possible structures need to be considered.

F4 ***(i) Bonding via the Fluorine.*** Figure 4 shows some of the starting structures that were employed to study the adsorption of the 7-TFA-NBE molecule on the Si(001) surface via one or more of its fluorine atoms. In Figure 4a, the 7-TFA-NBE molecule interacts with the silicon surface via a single fluorine atom, making a bond with one of the silicon dimer atoms. In Figure 4b, one of the fluorine atoms bridges across a silicon dimer. In Figure 4c, two fluorine atoms bond to a single silicon dimer atom, whereas in Figure 4d, a single fluorine atom bridges between two silicon dimer atoms from different dimers in the same dimer row. By varying the main bond lengths, bond angles, and dihedral angles, a number of different starting geometries based on the basic structures in Figure 4a−d were obtained. None of these starting geometries, however, were found to yield a stable structure.

(ii) Bonding via the Oxygen. To study the second scenario, we performed calculations for different structures that involved interaction of the molecule with the silicon surface via one of the oxygen atoms (O_2). Figure 5 shows two such starting F5 geometries. In the first structure (Figure 5a), the oxygen atom makes a single bond with one of the silicon dimer atoms, whereas in the second structure, (Figure 5b), the oxygen atom bridges across one of the silicon dimers.

Of these two starting geometries, only that in Figure 5a was found to yield a structure in which the 7-TFA-NBE molecule is bound to the surface. This structure is presented in Figure 6. F6 We observe that, although the molecule has remained intact, it has undergone considerable reorientation and rearrangement to

ohio2/yjy-yjy/yjy-yjy/yjy99907/yjy9839d07z | xppws | 23:ver.3 | 8/7/09 | 15:41 | Msc: jp-2009-03481w | TEID: ccd00 | BATID: 00000

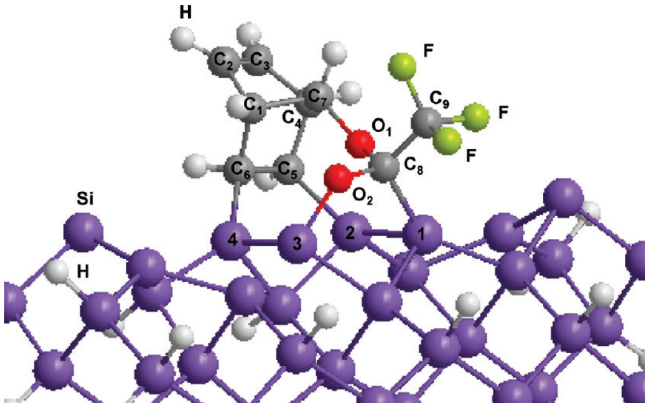

Figure 6. The optimized oxygen-bonded structure that results from the structure in Figure 5a.

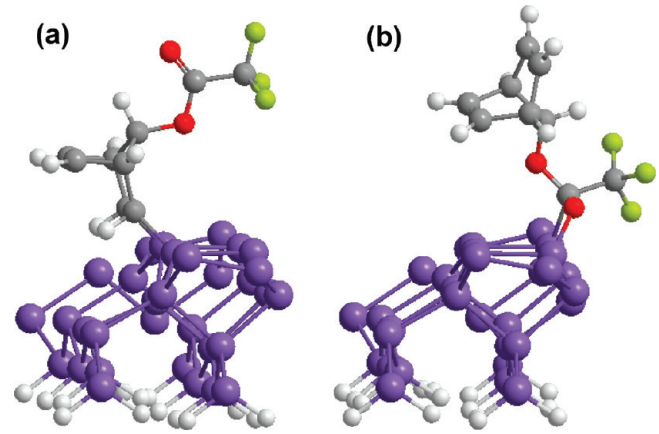

Figure 7. The optimized geometries for the (a) C_6-C_5 and (b) C_8-O_2 bonded structures.

allow the formation of four bonds with the silicon atoms of two adjacent dimers. In addition to the oxygen O_2, the new bonds involve the carbon atom C_8 and two of the carbon atoms in the NBE moiety (C_5 and C_6) (see Figure 6). Some of the bond lengths and bond angles defining the stable bonding configuration shown in Figure 6 are presented in Table 2. Comparison of these values with those for the isolated molecule (Table 1) reveals that some of the bond lengths and bond angles have changed significantly to allow this new bonding configuration to occur. The O_1-C_8 bond length predicted by the B3LYP/3-21G* Gaussian03 calculations, for example, has increased by 0.10 Å, and the $O_1-C_8-O_2$ bond angle has decreased by ~14° due to a change in the bonding configuration from sp^2 to the more tetrahedral sp^3. The C_8-O_2 and C_6-C_5 bond lengths are also now significantly longer due to the fact that these bonds have both become single bonds. Also presented in Table 2 are the structural parameters for this oxygen-bonded structure obtained from performing VASP calculations with a (4 × 4) SUC. We observe that the geometries predicted by Gaussian03 and VASP are quite similar, although there are some notable variations, such as in the C_8-Si_1 bond length and the $O_2-Si_3-Si_4$ bond angle. These variations are most likely due to the finite size of our Gaussian cluster and the imposition of periodic boundary conditions in the case of the VASP calculations. The binding energy of this oxygen-bonded structure was determined from our VASP calculations to be 2.81 eV.

There are several possible mechanisms for the formation of this oxygen-based structure. The most probable of these would be that the molecule first chemisorbs via the C_6 and C_5 atoms, forming bonds with the silicon atoms of two adjacent dimers, and then the molecule reorientates to form the required $Si-O_2$ and $Si-C_8$ bonds. Alternatively, the molecule first bonds via the O_2 and C_8 atoms and then reorientates to form the $Si-C_6$ and $Si-C_5$ bonds. We have investigated both of these possibilities and found that both of the intermediate C_6-C_5 and C_8-O_2 bonding structures are stable. These structures are shown in Figure 7a,b.

The binding energies of these two intermediate structures were determined to be 1.46 and 0.80 eV for the C_6-C_5 and C_8-O_2 configurations, respectively. Our value of 1.46 eV for the C−C bonded configuration is 0.36 eV smaller than the value of 1.82 eV obtained for the corresponding NBE bonding configuration by Bilic et al. (see panel 12, Figure 2, of ref 24). It is also smaller than the binding energies of 1.77 and 1.71 eV obtained by Bilic et al.[24] for ethylene and maleic anhydride bridge-bonded to Si(001) across the ends of two adjacent dimers through the formation of two Si−C bonds. To check the accuracy of our results, we also calculated the binding energy for the corresponding NBE intermediate structure. We obtained the value of 1.88 eV, in very good agreement with the 1.82 eV result of Bilic et al.[24] Thus, the C−C intermediate structure is relatively less stable for the 7-TFA-NBE molecule than for its NBE, ethylene, and maleic anhydride counterparts. The bond strength decreases as the electron-withdrawing power of the substituents increases, with the strongly electron withdrawing trifluoroacetoxyl group having the largest effect. Studies of the chemisorption of acetone on Si(001) have shown that bonding of the carbonyl (C═O) group across the ends of two adjacent

TABLE 2: Values of Some of the Bond Lengths (in Å) and Bond Angles (in Degrees) of the Oxygen-Bonded Structure Shown in Figure 6 Obtained from Our VASP and B3LYP/3-21G* Gaussian03 Calculations. The C_9-F Bond Length Has Been Averaged over the Three C−F Bonds

	C_1-C_2	$C_2=C_3$	C_1-C_7	C_7-O_1	O_1-C_8	C_8-O_2
VASP	1.52	1.34	1.55	1.45	1.42	1.41
G03	1.53	1.34	1.56	1.45	1.44	1.45
	C_8-C_9	C_6-C_5	$(C_9-F)_{avg}$	H_1-C_7	C_5-Si_2	C_8-Si_1
VASP	1.53	1.60	1.37	1.09	2.00	2.10
G03	1.51	1.63	1.38	1.09	1.98	1.99
	C_6-Si_4	O_2-Si_3	$C_7-O_1-C_8$	$O_1-C_8-O_2$	$C_8-Si_1-Si_2$	$O_2-Si_3-Si_4$
VASP	1.94	1.73	130.9	115.6	98.2	101.7
G03	1.94	1.72	130.8	113.2	96.3	107.5
	$C_5-Si_2-Si_1$	$C_6-Si_4-Si_3$	$Si_4-C_6-C_5$	$C_6-C_5-Si_2$	$Si_3-O_2-C_8$	$O_2-C_8-Si_1$
VASP	118.6	113.9	118.3	112.8	123.6	115.5
G03	123.8	113.2	117.4	111.1	119.5	118.2

ohio2/yjy-yjy/yjy-yjy/yjy99907/yjy9839d07z | xppws | 23:ver.3 | 8/7/09 | 15:41 | Msc: jp-2009-03481w | TEID: ccd00 | BATID: 00000

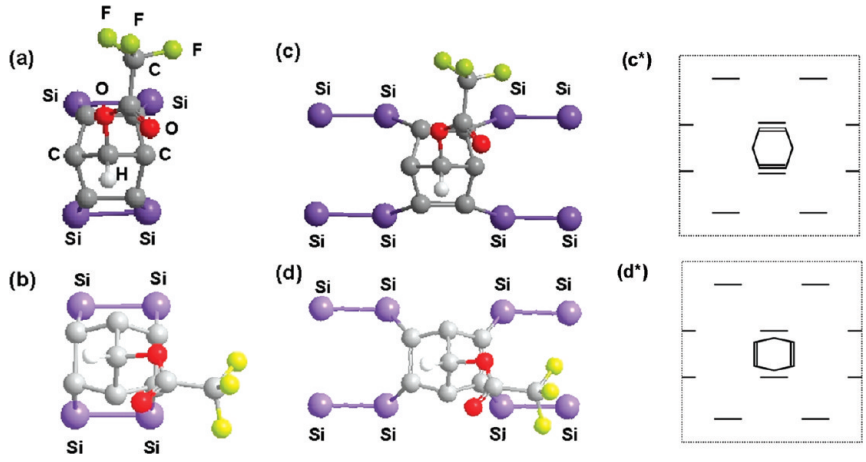

Figure 8. Possible structures for the interaction of the 7-TFA-NBE molecule with the Si(001) surface via the carbon atoms in the NBE unit: (a) the molecule within a dimer row with the C═C bonds oriented parallel to the silicon dimer bonds, (b) the molecule within a dimer row with the C═C bonds oriented perpendicular to the silicon dimer bonds, (c) the molecule between two dimer rows with the C═C bonds oriented parallel to the silicon dimer bonds, and (d) the molecule between two dimer rows with the C═C bonds oriented perpendicular to the silicon dimer bonds. The panels in (c*) and (d*) present schematics of the lowest-energy configurations that result from reorganization of the Si−Si dimers bonding to the molecule in (c) and (d), with the full lines indicating the Si−Si dimers.

Si−Si dimers produces stable structures analogous to our C_8-O_2 intermediate bonding structure (see Figure 3 of ref 46).

It is clear from the calculated binding energy values that the C_6-C_5 intermediate bonding structure is considerably lower in energy than the C_8-O_2 intermediate structure. However, this information is insufficient to determine which of the above two mechanisms, if either, is the correct one for forming the oxygen-bonded structure. To do this, we would need to calculate the activation energies associated with both the formation of these intermediate chemisorption structures from the gas phase and the subsequent reorientation of the molecule and formation of the remaining two bonds to yield the oxygen chemisorbed structure shown in Figure 6. Unfortunately, such calculations are extremely difficult and computationally expensive to perform.

(iii) Bonding via the Olefinic Carbon Atoms in the NBE Moiety. To study the adsorption via the olefinic sp^2-hybridized carbon atoms in the NBE moiety of the 7-TFA-NBE molecule, a number of different possible configurations were considered. These correspond to the C═C bonds being located above either a Si dimer row or a trough and being either parallel or perpendicular to the Si−Si dimer bonds. Figure 8 shows schematics of some of these possible structures.

To determine the optimized geometries of these structures and to compare them with the oxygen-bonded structure shown in Figure 6, we have employed the VASP periodic slab method with a (4 × 4) SUC. This is necessary as two of these structures involve two dimer rows and, hence, cannot be modeled by the single-dimer-row $Si_{36}H_{34}$ cluster employed in the earlier Gaussian03 calculations. Although all four of the structures shown in Figure 8 were found to be stable, reorganization of the Si−Si dimers in the case of Figure 8c,d led to the lower-energy configurations shown schematically in Figure 8c*,d*. Entirely similar results were found by Bilic et al.[24] for the interaction of NBE with Si(001). The four C-bonded structures (8a, 8b, 8c*, and 8d*) were found to be the lowest-energy structures for 7-TFA-NBE on the Si(001) surface. The structural parameters (i.e., the bond lengths and bond angles) obtained for these structures from our VASP calculations are shown in Table 3. The corresponding binding energy values are given in Table 4. These latter values show that the most stable configuration is the structure shown in Figure 8b where the molecule lies within a dimer row with the C═C bonds oriented perpendicular to the silicon dimer bonds. This minimum-energy structure is shown in Figure 9. The oxygen-bonded structure shown in Figure 6 is found to be less stable than all four of the lowest-energy carbon-bonded configurations.

Also presented in Table 4 are the binding energy values for the four corresponding NBE[24] and TMSAN[45] carbon-bonded structures. The relative stability of these four structures is seen to be essentially the same for all three molecules. In each case, the lowest-energy configuration is predicted to be configuration b, followed in order of decreasing stability by structures d*, a, and c*. This similarity of behavior is not surprising given that all of these molecules have the same NBE moiety. The relatively small differences between the binding energy values of the three molecules for a given bonding configuration can be readily accounted for by the somewhat different functional group that is attached to the NBE moiety in each case: the strongly electron-donating trimethylsilyl group increases the bond strength, whereas the strongly electron-withdrawing trifluoroacetoxyl group decreases the bond strength.

All of the above VASP calculations were performed using a slab containing four silicon layers. To test the reliability of this approach, we also analyzed the lowest-energy structure (Figure 8b) using six silicon layers and relaxing all of the atoms up to and including the third layer. The binding energy of the 7-TFA-NBE molecule on the Si(001) surface for this configuration was found to be 3.72 eV. Allowing the fourth layer of this six-layer slab to also relax resulted in this binding energy increasing to 3.77 eV. The corresponding value for the binding energy of the 7-TFA-NBE molecule on the Si(001) surface using four silicon layers and relaxing up to and including the third layer was 3.90 eV, as shown in Table 4. It follows that increasing the number of silicon layers from four to six only changes the binding energy value by 0.18 eV (<5%), whereas relaxing the additional fourth layer produces only a 0.05 eV (∼1%) variation. These energy differences are clearly too small to change the predicted stability ordering of these structures.

To confirm the reliability of our structural parameters for the lowest-energy 7-TFA-NBE configuration, we set up this chemisorption structure (Figure 8b) on the substrate geometry shown in Figure 3a and then optimized its geometry using Gaussian03 with B3LYP/3-21G*. The bond lengths and bond angles obtained from this latter optimization were found to be in very

TABLE 3: Bond Length and Bond Angle Values Obtained from Our VASP Calculations for the Four Lowest-Energy Carbon-Bonded Structures (see Figure 8) and the Oxygen-Bonded Structure Presented in Figure 6

	$(\text{dimer bond})_{\text{avg}}$[a]	$(\text{dimer}-\text{dimer})_{\text{avg}}$[a]	$(\text{Si}-\text{C})_{\text{avg}}$[a]	C_1-C_2	C_2-C_3	C_1-C_7
8a	2.36	3.58	1.95	1.56	1.60	1.56
8b	2.37	3.38	1.96	1.56	1.61	1.54
8c*	2.37	3.60	1.95	1.56	1.60	1.56
8d*	2.38	3.40	1.96	1.56	1.62	1.54
via O	2.38	3.33	1.97	1.52	1.34	1.55
C_7-O_1	O_1-C_8	$C_8=O_2$	C_8-C_9	$(C_9-F)_{\text{avg}}$[a]	H_1-C_7	
8a	1.47	1.34	1.21	1.57	1.36	1.09
8b	1.47	1.34	1.21	1.56	1.36	1.09
8c*	1.47	1.34	1.21	1.57	1.36	1.09
8d*	1.47	1.34	1.21	1.56	1.36	1.09
via O	1.45	1.42	1.41	1.53	1.37	1.09
$C_1-C_2-C_3$	$C_6-C_1-C_2$	$C_7-O_1-C_8$	$O_1-C_8-O_2$	$O_2-C_8-C_9$	$O_1-C_8-C_9$	
8a	103.2	118.3	120.9	129.5	122.1	108.1
8b	102.0	110.6	118.8	129.5	122.2	108.6
8c*	103.1	118.1	120.9	129.5	122.2	108.0
8d*	102.1	110.4	118.9	129.2	122.3	108.4
via O	107.7	104.4	130.9	115.6	108.3	109.9
$H_1-C_7-O_1$	$O_1-C_7-C_1$	$O_1-C_7-C_4$	$C_1-C_7-C_4$	$C_1-C_2-\text{Si}$	$C_3-C_2-\text{Si}$	
8a	109.3	112.2	108.1	95.3	125.6	100.3
8b	109.5	111.2	107.6	95.4	109.2	117.8
8c*	109.3	112.2	108.1	95.4	125.5	101.2
8d*	109.6	111.2	107.5	95.5	109.1	117.6
via O	110.8	119.7	103.3	94.3		

[a] The values denoted by "avg" have been obtained by averaging either over all of the dimers adjacent to the chemisorbed molecule or over all of the Si−C or C−F bonds.

TABLE 4: Binding Energies (in eV) for the Adsorption of the NBE,[24] TMSAN,[45] and 7-TFA-NBE Molecules on the Si(001) Surface Obtained Using VASP. Values Are Presented for the Four Lowest-Energy C-Bonded Structures (see Figure 8) and the Oxygen-Bonded Structure (Figure 6)

molecule	8a	8b	8c*	8d*	via the O
NBE	3.51	4.16	3.12	3.68	
TMSAN	3.94	4.55	3.59	4.07	
7-TFA-NBE	3.25	3.90	3.12	3.59	2.81

good agreement with the VASP values, with the maximum difference being only 2%.

D. Activation Barrier. To determine how readily the structure shown in Figure 8b might form on the Si(001) surface, we have calculated the reaction path between the chemisorbed (minimum-energy) structure and the physisorbed state. To do this, we have used the nudged elastic band (NEB) method contained within the VA,SP program. Sixteen images were employed between these initial and final states, and the calculations were continued until the total energy had converged to the specified accuracy. The resultant energy curve is shown in Figure 10. We observe that the maximum lies 0.23 eV above the energy of the physisorbed state. The activation energy for the adsorption of the 7-TFA-NBE molecule on Si(001) in Figure 8b is thus predicted to be ≤0.23 eV. This is to be compared with the value of ∼0.10 eV determined for the corresponding NBE structure by Bilic et al.[24] Both of these activation energies are small, which suggests that both structures would readily form on the Si(001) surface.

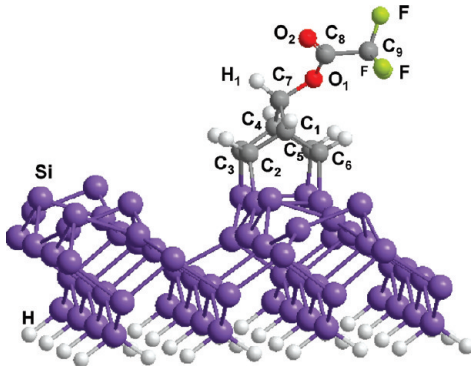

Figure 9. Side view of the minimum-energy structure in Figure 8b. The C=C double bonds in the molecule are between C_2 and C_3, and between C_5 and C_6.

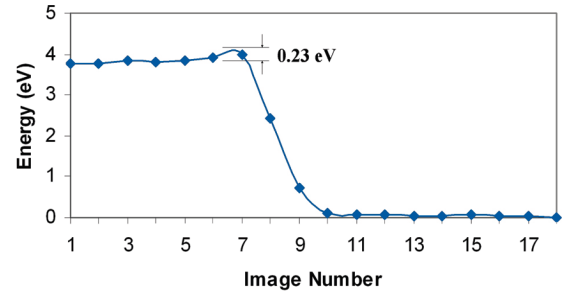

Figure 10. Plot of energy versus image number for the adsorption of the 7-TFA-NBE molecule on the Si(001) surface from the physisorbed state for the configuration in Figure 8b.

E. Possible Dissociative Reactions of 7-TFA-NBE on the Silicon Surface. The reactivity of the silicon surface is such that many types of single bonds in molecules will break, allowing for the formation of two dissociation-product fragments on the surface or the abstraction of atom pairs with multiple bonds forming in the remnant molecule. As NBE itself reacts with the surface without displaying any of these types of processes, the C−C, C=C, and C−H bonds in the molecule are stable. Carbonyl bonds in ketones are known to only react with the Si(001) surface to produce simple adducts,[18] and as the bond strengths of C=O bonds in ketones and esters are very

ohio2/yjy-yjy/yjy-yjy/yjy99907/yjy9839d07z | xppws | 23:ver.3 | 8/7/09 | 15:41 | Msc: jp-2009-03481w | TEID: ccd00 | BATID: 00000

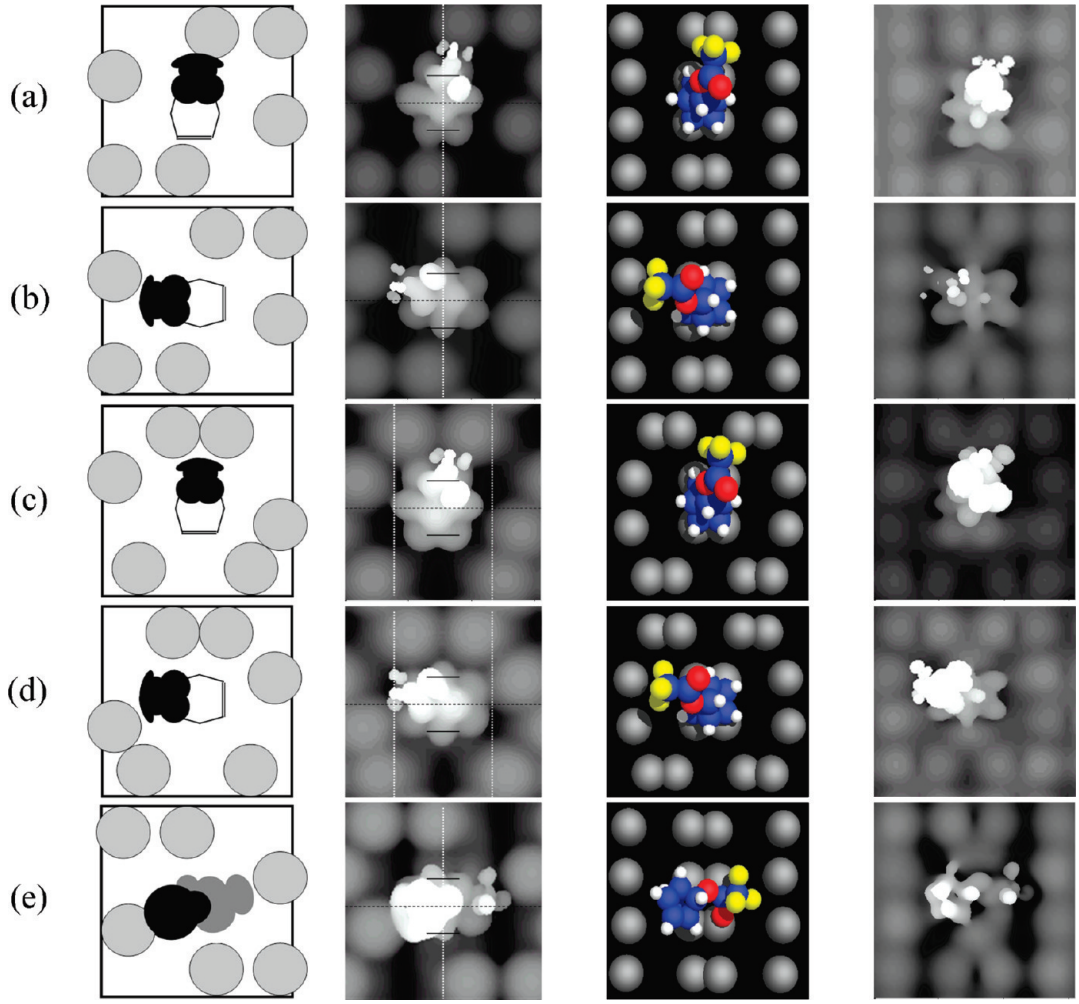

Figure 11. Simulated STM filled-state images (second column) and empty-state images (fourth column) for the (a−d) four lowest-energy carbon-bonded structures and (e) the oxygen-bonded structure. The filled-/empty-state images have been obtained by integrating over a range of −2.0/+2.0 eV from the Fermi energy, and the isosurface value is 4.2×10^{-4} e/Å^3. The white vertical dotted lines in the second column indicate the middle of the dimer rows, whereas the black horizontal dashed lines indicate midway between the chemisorbed dimers. The short, black solid lines denote the two Si−Si dimers directly involved in the chemisorption of the molecule. In the third column top views, the atoms are colored red (oxygen), blue (carbon), yellow (fluorine), and white (hydrogen). The first column presents schematics of the expected filled-state images following rotational averaging, with the gray circles representing the up-Si dimer atoms and the dark section the main protrusion due to the 7-TFA-NBE molecule.

similar,[47] analogous behavior is expected for 7-TFA-NBE. Without activation processes, C−O single bonds are very stable as their bond strengths are large: 4.4 and 4.0 eV for the C(O)−O and C(O)O−C bonds of methyl acetate $CH_3C(O)OCH_3$, respectively;[47] DFT calculations (at the B3LYP/6-31+G* level) indicate that these energies increase further by 0.08 and 0.27 eV, respectively, upon substitution of the electron-withdrawing trifluoro group to make $CF_3C(O)OCH_3$. In principle, the silicon surface itself could provide heterogeneous catalysis of the cleavage of these bonds, but the bonds themselves are sterically shielded from the surface. Any interaction of the surface with the exposed carbonyl group is likely to further stabilize the C−O single bonds. Hence, these bonds are not expected to be reactive. The only other bonds present in 7-TFA-NBE are the C−F bonds. Although such bonds have been shown to dissociate on the Si(001) surface, studies of the interaction of halogen-substituted benzene and ethylene molecules with Si(001) have shown that, whereas the C−Cl and C−Br bonds dissociated, the C−F bonds remained intact.[48] This is no doubt due to the greatly increased strength of the C−F bonds (5.1 eV compared with 3.5 and 2.9 eV, respectively).[47]

The simulations described previously could all, in principle, lead to dissociative reactions of 7-TFA-NBE, but no such processes were found. This indicates that the barriers for these processes are larger than those for simple adduct-forming reactions. As the barriers for the adduct-forming reactions have been shown to be very small and as the bond energies for breaking the C−O and C−F single bonds are quite large, dissociative reactions of 7-TFA-NBE with the surface are not expected. Subsequent dissociation of the different resultant adduct structures could, of course, occur at elevated temperatures, but such reactions are outside the focus of the present study.

F. Simulated STM Images. One of the main aims of this work is to ascertain whether the actual bonding configurations of the 7-TFA-NBE molecule on the Si(001) surface could be determined using STM. As a result, we have simulated STM images for our four lowest-energy carbon-bonded structures shown in Figure 8 and the oxygen-bonded structure shown in Figure 6. The resultant filled-state and empty-state images are presented in Figure 11 and have been obtained by integrating over a range of ±2.0 eV from the Fermi energy and employing an isosurface value of 4.2×10^{-4} e/Å^3. In all of the filled-state images, the up-buckled silicon atoms are reasonably bright, whereas the down-buckled silicon atoms are dark. In the empty-state images, both the up- and the down-buckled silicon atoms

have similar intensities. The images for some of the structures exhibit protrusions above a dimer row (Figure 11a,b,e), whereas in others (Figure 11c,d), the protrusions due to the absorbate lie over a trough between two dimer rows. The distributions of the bright regions resulting from the up-Si dimer atoms are also distinctly different in these two cases. All of the images exhibit some asymmetry about the center of the dimer row or trough where the molecule is chemisorbed.

Of particular significance is the fact that the CF_3 component of the 7-TFA-NBE molecule can be clearly identified in all of the filled-state images (as well as most of the empty-state images), with the $C-CF_3$ moiety being oriented either along the dimer row or perpendicular to the dimer rows. All of these considerations suggest that these different structures should be distinguishable in STM. Of course, free rotation of the CF_3 group of the molecule, and flipping of the trifluoroacetoxy "arm" of the molecule between its two conformer configurations for the four C-bonded structures, will produce significant broadening of the features shown in the simulated images of Figure 11 (each of which is for one particular configuration). However, rotation of the CF_3 group will simply transform the three bright spots arising from the F atoms into a band. Moreover, rotation to the other conformer will not change the orientation of the main protrusion with respect to the dimer rows. As an indication of the effects of all possible motions on the time scale of the STM measurement, schematics of the expected time-averaged filled-state STM images are provided alongside the actual single-configuration simulated filled-state images in columns 1 and 2 of Figure 11. From these schematics it is clear that all of the likely bonding scenarios should be identifiable on the surface. As indicated earlier, such discrimination is not possible for more symmetrical adsorbate molecules, such as NBE. Significant differences between the corresponding empty-state images are also apparent from the simulated images in column 4.

4. Conclusions

The adsorption of 7-TFA-NBE on the Si(001) surface has been studied using three possible chemisorption scenarios: (1) binding of the molecule to the surface via the fluorine, (2) binding through the oxygen atoms, and (3) binding through the carbon atoms. As expected, binding through the fluorine atoms was not possible, whereas binding through the carbon atoms occurred analogously to that for NBE. However, a binding scenario was also found in which the adsorbate forms bonds with the four silicon atoms of two adjacent dimers in the same dimer row of the Si(001) surface, with one of these bonds being a Si−O bond, whereas the other three are Si−C bonds. All of these structures were found to have large binding energies, indicating that they were all very stable structures.

The lowest-energy adsorbate structure is predicted to be that in which the 7-TFA-NBE molecule lies erect within a dimer row with the C═C bonds oriented perpendicular to the silicon dimer bonds. The activation energy for the formation of this structure was predicted to have an upper bound of only 0.23 eV, indicating that this structure will readily form. The other carbon-bonded structures are less stable by 0.31−0.78 eV. The extent to which these structures will also be formed on the Si(001) surface will be determined by the corresponding activation barriers and the temperature. The O-bonded structure has been predicted to be of significantly higher energy than all of the C-bonded structures. The adsorption, however, is controlled by kinetic rather than thermodynamic factors, and hence, O-bonded structures on the surface may also occur.

It has also been shown that the simulated images for the different possible chemisorption structures of a 7-TFA-NBE molecule on the Si(001) surface are clearly distinguishable, even when rotational averaging effects are included. This is a very significant result as it indicates that high-resolution STM measurements of the 7-TFA-NBE exposed Si(001) surface should enable us to determine which of these theoretically predicted structures actually occur on the surface. The demonstration that the bonding configuration of molecules, such as 7-TFA-NBE on Si(001), could be determined via STM is of fundamental importance to the development of molecular electronics where precise knowledge of the placement and orientation of the molecules making up each component of a device is essential. Precise knowledge of the bonding structures on a given surface is also foundational to understanding how unwanted structures could be eliminated and the surface modified to achieve a specific functionality.

Finally, comparison of the calculated structure of the isolated 7-TFA-NBE molecule with the predicted carbon-bonded structures of this molecule on the Si(001) surface indicates that the $OC(O)CF_3$ component of the chemisorbed molecule sits well above the surface and has a structure very close to that of the isolated molecule. As a result, we would, therefore, expect the functionality of this molecule on the Si(001) surface for the carbon-bonded structures to be very similar to that of the $OC(O)CF_3$ group of the isolated molecule. In addition, we would expect other norbornadiene-based molecules to similarly bond via their norbornadiene moiety with their functional groups positioned above the surface. On the basis of the current work, these structures should be experimentally distinguishable within STM. Moreover, the response of these molecular structures to an applied electric field or current, for example, could be varied by changing their functional group. Employing different norbornadiene-based molecules thus offers a well-defined pathway for producing very stable, experimentally verifiable molecular structures on Si(001) whose properties could be readily tailored for specific atomic-scale applications.

Acknowledgment. S.A.S. acknowledges Al-Hussein Bin Talal University in Ma'an, Jordan, for their award of a scholarship, whilst M.J.C. and J.R.R. acknowledge research funding from the Australian Research Council (Discovery Project Grant DP0773847). The Australian Partnership for Advanced Computing (APAC) is also acknowledged for the award of supercomputer processing time under their Merit Allocation scheme.

References and Notes

(1) Rakshit, T.; Liang, G. C.; Ghosh, A. W.; Datta, S. *Nano Lett.* **2004**, *4*, 1803.
(2) Wolkow, R. A. *Annu. Rev. Phys. Chem.* **1999**, *50*, 413.
(3) Hamers, R. J.; Coulter, S. K.; Ellison, M. D.; Hovis, J. S.; Padowitz, D. F.; Schartz, M. P.; Greenlief, C. M.; Russel, J. N., Jr. *Acc. Chem. Res.* **2000**, *33*, 617.
(4) Filler, M. A.; Bent, S. F. *Prog. Surf. Sci.* **2003**, *73*, 1.
(5) Ma, Z.; Zaera, F. *Surf. Sci. Rep.* **2006**, *61*, 229.
(6) Leftwich, T. R.; Teplyakov, A. V. *Surf. Sci. Rep.* **2008**, *63*, 1.
(7) Hersam, M. C.; Guisinger, N. P.; Lyding, J. W. *Nanotechnology,* **2000**, *11*, 70.
(8) Liu, Q.; Hoffmann, R. *J. Am. Chem. Soc.* **1995**, *117*, 4082.
(9) Hamers, R. J.; Hovis, J. S.; Lee, S.; Liu, H.; Shan, J. *J. Phys. Chem. B* **1997**, *101*, 1489.
(10) Hovis, J. S.; Liu, H. B.; Hamers, R. J. *J. Phys. Chem. B* **1998**, *102*, 6873.
(11) Witkowski, N.; Hennies, F.; Pietzsch, A.; Mattsson, S.; Fohlisch, A.; Wurth, W.; Nagasono, M.; Piancastelli, M. N. *Phys. Rev. B* **2003**, *68*, 115408.
(12) Barriocanal, J. A.; Doren, D. J. *J. Am. Chem. Soc.* **2001**, *123*, 7340.
(13) Li, Q.; Leung, K. T. *Surf. Sci.* **2003**, *541*, 113.
(14) Qiao, M. H.; Tao, F.; Cao, Y.; Xu, G. Q. *Surf. Sci.* **2003**, *544*, 285.

(15) Wang, G. T.; Mui, J. F.; Tannaci, J. F.; Filler, M. A.; Musgrave, C. B.; Bent, S. F. *J. Phys. Chem. B* **2003**, *107*, 4982.
(16) Huang, H. G.; Zhang, Y. P.; Cai, Y. H.; Huang, J. Y.; Yong, K. S.; Xu, G. Q. *J. Chem. Phys.* **2005**, *123*, 104702.
(17) Huang, H. G.; Huang, J. Y.; Cai, Y. H.; Xu, G. Q. *Chem. Phys. Lett.* **2005**, *414*, 143.
(18) Saraireh, S. A.; Smith, P. V.; Radny, M. W.; Schofield, S. R.; King, B. V. *Surf. Sci.* **2008**, *602*, 3484.
(19) Pitters, J. L.; Wolkow, R. A. *Nano Lett.* **2006**, *6*, 390.
(20) Yokozeki, A.; Kuchitsu, K. *Bull. Chem. Soc. Jpn.* **1971**, *44*, 2356.
(21) Hersam, M. C.; Guisinger, N. P.; Lyding, J. W. *Nanotechnology* **2000**, *11*, 70.
(22) Abeln, G. C.; Lee, S. Y.; Lyding, J. W.; Thompson, D. S.; Moore, J. S. *Appl. Phys. Lett.* **1997**, *70*, 2747.
(23) Abeln, G. C.; Hersam, M. C.; Thompson, D. S.; Hwang, S.-T.; Choi, H.; Moore, J. S.; Lyding, J. W. *J. Vac. Sci. Technol., B* **1998**, *16*, 3874.
(24) Bilic, A.; Reimers, J. R.; Hush, N. S. *J. Chem. Phys.* **2003**, *119*, 1115.
(25) Hovis, J. S.; Lee, S.; Liu, H.; Hamers, R. J. *J. Vac. Sci. Technol., B* **1997**, *15*, 1153.
(26) Hovis, J. S.; Liu, H.; Hamers, R. J. *Appl. Phys. A: Mater. Sci. Process.* **1998**, *66*, S553.
(27) Matrisciano, R.; Snyder, W. H. *J. Chem. Eng. Data* **1971**, *16*, 490.
(28) Dal Bola, L.; De Amici, M.; De Micheli, C.; Gandolfi, R.; Houk, K. N. *Tetrahedron Lett.* **1989**, *30*, 807.
(29) (a) Kresse, G.; Hafner, J. *Phys. Rev. B* **1993**, *47*, 558. (b) Kresse, G.; Hafner, J. *Phys. Rev. B* **1994**, *49*, 14251.
(30) Kresse, G.; Furthmuller, J. *Comput. Mater. Sci.* **1996**, *6*, 15.
(31) Kresse, G.; Furthmuller, J. *Phys. Rev. B* **1996**, *54*, 11169.
(32) Foresman, J. B.; Frisch, Æ. *Exploring Chemistry with Electronic Structure Methods*, 2nd ed.; Guassian, Inc.: Pittsburgh, PA, 1995−1996.
(33) Vanderbilt, D. *Phys. Rev. B* **1990**, *41*, 7892.
(34) Kresse, G.; Hafner, J. *J. Phys.: Condens. Matter* **1994**, *6*, 8245.
(35) Perdew, J. P.; Wang, Y. *Phys. Rev. B* **1992**, *45*, 13244.
(36) Perdew, J. P.; Chevary, J. A.; Vosko, S. H.; Jackson, K. A.; Pederson, M. R.; Singh, D. J.; Fiolhais, C. *Phys. Rev. B* **1992**, *46*, 6671.
(37) Monkhorst, H. J.; Pack, J. D. *Phys. Rev. B* **1976**, *13*, 5188.
(38) Becke, A. D. *J. Chem. Phys.* **1993**, *98*, 5648.
(39) Tersoff, J.; Hamann, D. R. *Phys. Rev. Lett.* **1983**, *50*, 1998.
(40) Tersoff, J.; Hamann, D. R. *Phys. Rev. B* **1985**, *31*, 805.
(41) Weast, R. C., Ed. *Handbook of Chemistry and Physics*, 55th ed.; CRC Press: Cleveland, OH, 1974−1975.
(42) Edwards, J. G.; Franklin, H. F.; Gilles, P. W. *J. Chem. Phys.* **1971**, *54*, 545.
(43) Sanderson, R. T. *Chemical Bonds and Bond Energy*; Academic Press: New York, 1971.
(44) Darwent, B. deB. *Bond Dissociation Energies in Simple Molecules*; U.S. Government Printing Office: Washington, DC, 1970.
(45) Wang, B.; Zheng, X.; Michl, J.; Foley, E. T.; Hersam, M. C.; Bilic, A.; Crossley, M. J.; Reimers, J. R.; Hush, N. S. *Nanotechnology* **2004**, *15*, 324.
(46) Warschkow, O.; Gao, I.; Schofield, S. R.; Belcher, D.; Radny, M. W.; Saraireh, S. A.; Smith, P. V. *Phys. Chem. Chem. Phys.* **2009**, *11*, 2747.
(47) Luo, Y. R. *Comprehensive Handbook of Chemical Bond Energies*; Taylor & Francis: Boca Raton, FL, 2007.
(48) Zhou, X. J.; Leung, K. T. *Surf. Sci.* **2006**, *600*, 3285.

JP903481W